

## Two Dimensional Infrared Spectroscopy: Studies of the Dynamics of Structures with Femtosecond Pulse Fourier Transform Correlation Spectroscopy

Robin. M. Hochstrasser,\* Nien-Hui Ge, Sandrasegaram Gnanakaran, and Martin T. Zanni

Department of Chemistry, University of Pennsylvania, Philadelphia, PA 19104-6323, USA

(Received October 31, 2001)

Features of heterodyned infrared photon echo experiments that generate two and three dimensional infrared spectra are described. The relationship of these spectra to structures, correlated fluctuations, energy transfer and orientational motions are illustrated with experimental and simulated examples.

The experimental realization of 2D IR occurred during the past four years, first in a pump-probe configuration,<sup>1–3</sup> and then in a heterodyned version, which is operationally more akin to pulsed NMR.<sup>4–9</sup> Theories of multidimensional optical<sup>10,11</sup> and more recently IR nonlinear methods<sup>12,13</sup> and related experimental works on coherent methods<sup>14–17</sup> represent parallel approaches. This is a rapidly growing area of research: the 2D IR experiment is now being applied by other groups using both the pump-probe<sup>18–20</sup> and the heterodyned spectral interferometry approaches.<sup>21</sup> The work on peptides is complemented by theoretical simulations of the 2D IR of small peptides.<sup>22,23</sup> Combined optical-infrared approaches<sup>24</sup> are also being applied to vibrational coupling problems. The method of 2D IR has applications in many fields of molecular structure and dynamics besides biology: polymers, surfaces and liquid state dynamics are a few of the most prominent examples.

We have applied 2D IR to the amide I region of small peptides and proteins in the 1550–1700 cm<sup>−1</sup> region because of the well-known sensitivity of this mode to secondary structure. Extension to larger systems and different wavelength regions can now be expected.<sup>25</sup> In principle, the entire frequency range available to FTIR can be scanned in these types of experiments to obtain data sets in three frequency dimensions, thereby significantly enlarging the structural information content. Although the ideal structural method would measure atomic positions in molecules of arbitrary size and permit visualization of the structures throughout the course of conformational changes or chemical reactions, regardless of the time scales involved, no single experimental technique is likely to yield all of this information. However, 2D IR can certainly complement other approaches. Fourier transform infrared spectroscopy can monitor protein secondary structure features on the nanosecond to second timescale.<sup>26</sup> Pulsed IR methods can probe the vibrations of proteins on time scales down to the femtosecond regime.<sup>27–30</sup> The 2D IR spectroscopy incorporates both of these advantages in addition to showing promise for monitoring distributions of complex molecular assemblies evolving on hitherto unprecedented time scales.

Linear IR spectroscopy provides the fingerprints of the nu-

clear motions. In proteins, the amide I band is particularly sensitive to the secondary structure. The main contribution to the amide I band is from the carbonyl stretch.<sup>31,32</sup> The structure sensitivity of the amide I band arises from the frequency shift caused by external/internal hydrogen bonding of C=O, and the electrostatic coupling of neighboring units.<sup>33–39</sup> Utilization of linear IR spectra to deduce structures of proteins and peptides has been limited because of the congestion from overlapping amide I bands associated with different structural domains, and the differentiation of electrostatic interactions and energy shifts from environmental fluctuations. Experimental methods based on nonlinear IR spectroscopy can overcome many of those shortcomings by spreading out the spectra into more frequency dimensions. Two-dimensional infrared (2D IR) spectroscopy has emerged as a powerful approach to determine the dynamics of structures.<sup>4–7,11</sup> Its potential stems from the intrinsically versatile time resolution and spectral line narrowing capability combined with the ease of isotope editing different pieces of peptide structures. Thus, 2D IR spectroscopy naturally accesses time scales that are hard to attain by 2D NMR and X-ray diffraction methods in liquids. A recent issue of *Chemical Physics* contains articles about multidimensional spectroscopies now being developed.<sup>40</sup>

The important advance is the use of a heterodyned photon echo method to provide optimal spectral resolution by eliminating the inhomogeneous broadening in the infrared spectrum. Both two-pulse<sup>41</sup> and three-pulse IR photon echoes<sup>42,43</sup> of vibrations have been studied previously, but in these reported echo experiments the generated third order field alone creates a signal on a square law detector. This approach has two disadvantages: it is insensitive to the phase of the signal which provides optimized spectral information; and it decays at least twice as fast as the heterodyned signal, limiting the time scales during which vibrational dynamics can be observed. Spectral resolution of the generated vibrational echo field<sup>44–46</sup> permits some phase relations to be obtained, but does not yield line-narrowed spectra. However, the complete generated field amplitude and phase, free from any static inhomogeneous broadening, can be obtained in principle by means of heterodyne

echoes or spectral interferometry techniques. Such realization towards complete characterization of generated fields has been demonstrated for optical transitions<sup>16</sup> and for infrared transitions.<sup>4</sup>

### Principles of 2D IR Spectroscopy

Multidimensional methods have proved to be invaluable for simplifying and allowing more detailed interpretation of NMR spectra. The 2D IR spectrum, like NMR, can be generated by both multiple time or frequency domain methods. It was first reported as a frequency domain experiment<sup>1</sup> analogous to NMR double resonance, in which the vibrational excitations were excited by a narrow band IR pulse and probed by a broad band of infrared frequencies. A simple coupling model<sup>31,32</sup> reproduced the experimental 2D IR spectra. In these 2D IR spectra, coupled vibrational modes exhibited cross peaks that depended on the system's secondary and tertiary structure. Recently, infrared pulse sequences that are the direct analogs of those used in the COSY (correlation spectroscopy) and NOESY (nuclear Overhauser effect spectroscopy) methods of pulsed NMR have been used to perform 2D IR experiments.<sup>4,5,7</sup> These pulse sequences manipulate the vibrational coherences rather than the nuclear spins.

Heterodyned two-pulse IR correlation spectroscopy, which we will refer to as IR-COSY, has the same measurement principles as NMR COSY. In both techniques there is a preparation and a coherence transfer step (see Fig. 1). The first infrared pulse in 2D IR creates a vibrational coherence analogous to the spin coherence created by the first radio frequency pulse in NMR, but it does this with a weak interaction not a  $\pi/2$  pulse. After some delay, a pair of weak infrared pulses interrupts this initial coherence evolution to generate a free induction decay (FID) from the transferred coherence. The electric field of the

FID is the measured signal in both techniques. When the third IR pulse follows some time after the second one, the pulse sequence is analogous to NMR NOESY or a stimulated spin echo. We will refer to this experiment as THIRSTY (for Three infrared pulse stimulated echo spectroscopy). The variable delay between the second and third pulses allows time for vibrational coherence and population transfer to occur, analogous to spin transfer in NMR. The signals in the 2D IR experiments are created by the responses of the network of vibrational modes excited by the pulses, and can be spatially separated and independently measured from the transmitted fields by judicious choice of the input beam directions (see Fig. 1). Such spatial selection of phase is not possible in NMR because of the long wavelength of radio frequency fields. The vibrational FID is measured as a function of the three time intervals and yields a 3D time grid whose Fourier transforms give the IR-COSY and THIRSTY spectra. The diagonal peaks in these spectra correspond to the vibrational frequencies in the structure distribution, but the cross peaks show up only if the modes are coupled. Furthermore, the correlated motions of different parts of the molecule are also extractable from the IR-COSY spectra.<sup>9</sup> To obtain well-resolved 2D IR spectra, the FID periods need only to be measured for a few tens of picoseconds, thus the method can be used to monitor the structures of intermediates in kinetics experiments. Some typical FID signals

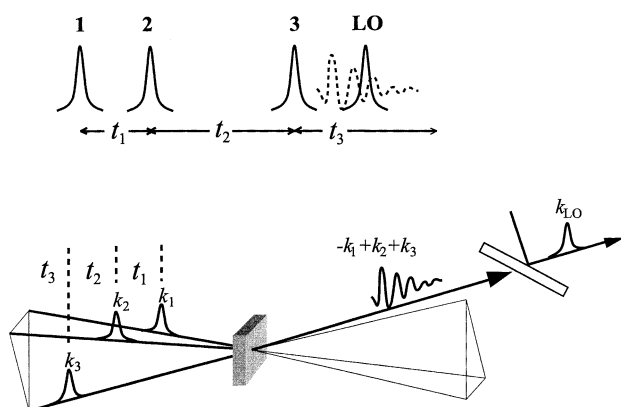


Fig. 1. Typical pulse sequences used in heterodyned 2D-IR spectroscopy. The three pulses are separated by the time delays  $t_1$  and  $t_2$ , and the free induction decay is measured versus  $t_3$ . In heterodyned 2D IR, the three infrared laser beams and the emitted FID signal beams all travel in different directions, and thus are spatially separated from one another. The electric field of the signal beam cannot be measured directly as it is in NMR, so it is overlapped with a fourth local-oscillator beam that heterodynes the signal. When  $t_2 = 0$ , the 2D IR spectrum is analogous to the NMR COSY experiment, otherwise it is similar to NOESY.

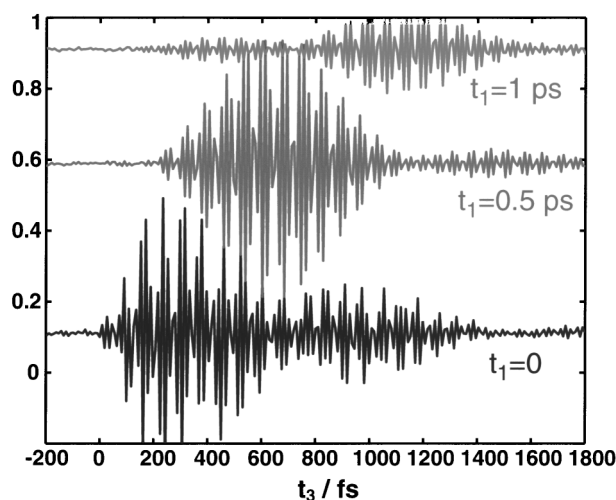


Fig. 2. The free induction decay (FID) or photon echo measured for the  $^{13}\text{C}$  isotope labeled peptide Ac-AAAA-KAAAAKAAAAAY-NH<sub>2</sub>. Each FID is generated with the labeled  $t_1$  and  $t_2 = 0$  as a function of  $t_3$  (see Fig. 1). The fast oscillations have a  $\sim 20$  fs period that is determined by the fundamental frequency of the amide I band, and the modulation in the signal is a result of the frequency separation between the  $^{12}\text{C}$  and  $^{13}\text{C}$  labeled amide groups. The signal peaks at later  $t_3$  for larger  $t_1$ . This is a clear signature that the peptide is inhomogeneously broadened, e.g. there is a distribution of structures that does not evolve on the timescale of the experiment. The data around  $-200$  fs illustrates the excellent signal to noise achievable in these heterodyned experiments. A 2D IR spectrum is generated by calculating the two-dimensional Fourier transform for a grid of FID data points.

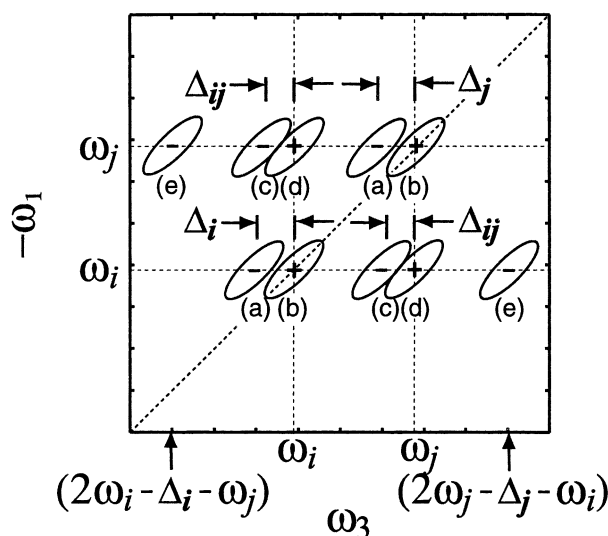


Fig. 3. Schematic diagram of the 2D IR spectrum for a two vibrator system. For each oscillator  $i$ , there are five peaks along the  $\omega_3$  axis at  $-\omega_1 = \omega_i$ . Peaks are labeled with “+” and “-” to designate the sign of their intensity in the real portion of the spectra. The peaks labeled (a) and (b) are diagonal peaks and are separated by the diagonal anharmonicity  $\Delta_i$  or  $\Delta_j$ . The peaks labeled (c) and (d) are cross-peaks that are separated by the off-diagonal anharmonicity  $\Delta_{ij}$ , which is determined by the structure of the molecule. The remaining peaks at (e) {and also at (a)} are forbidden in the extremely weak coupling limit. All peaks are elongated along the diagonal, which would occur for correlated inhomogeneously broadened systems.

seen in these experiments are shown in Fig. 2. A 2D Fourier transform is performed to generate the 2D IR spectrum from the time-domain data.

In general the fast oscillations and slow modulation of the FID signals arise from the fundamental vibrational period of the vibrators and their frequency separations. For  $\alpha$ -helical and other peptides or small proteins, individual amides have similar environments and frequency separations are small. Isotope substitution can rectify this problem in 2D spectroscopy. As shown in Fig. 2 the FID signals exhibit slow modulations of  $\sim 800$  fs when 4 of the 20 residues of an  $\alpha$ -helical peptide are  $^{13}\text{C}$  labeled. The  $\sim 35\text{ cm}^{-1}$  frequency shift of these selected amide modes allows their coupling to the unsubstituted amides to be measured.

When a realistic distribution of structures is used to simulate the 2D IR spectra, the peaks in the spectra become spread along the diagonal to form elliptical profiles (Fig. 3). The cross peaks also broaden into shapes dependent on the interactions between the peptide units and the relative motions of the coupled units. The minor axes of these ellipses are mainly determined by the dephasing of the vibrational modes. Thus, the distribution of peptide structures and their nuclear motions are reflected in the shapes and frequencies of the diagonal and cross-peaks.

### Vibrational Dynamics

The dynamics of vibrational excitations are a key part of the

interpretation of 2D IR spectra, much in the same way that spin dynamics have an essential role in NMR and EPR. However, the population relaxation times and dynamics of inhomogeneous distributions of vibrational frequencies are in the picosecond and subpicosecond regime at ambient temperatures and therefore ultrafast methods are needed to examine them. The ultimate spectral resolution is thereby shifted into a different regime. There has been considerable work on both the theory and experimental measurement of population and pure dephasing relaxation of molecules in solutions. In as much as these processes limit the spectral resolution of 2D IR spectroscopy, it is necessary that they are understood as well as possible. There is still not a reliable predictive theory for population relaxations, particularly when the energy is induced by solvent fluctuations to flow through both solvent modes and internal modes of the molecule under consideration.<sup>47–49</sup> In peptides containing a number of amide units, the spatial distributions of vibrational relaxation times and energy transfer between the various quasidegenerate modes have not been widely studied and the mechanisms of relaxation and energy transfer remain unclear. The pure dephasing processes in such molecules can also depend on the spatial location in the molecule of the relaxing group, and on the couplings between the sets of modes. Clearly a wide range of challenging questions are waiting to be answered by these new two dimensional techniques.

### Determination of Peptide Structures

The first detailed experimental application of IR-COSY on a coupled system was on the acetylproline- $\text{NH}_2$  dipeptide.<sup>7</sup> The real and absolute magnitude parts of the spectrum generated from the FID are shown in Fig. 4 for acetylproline- $\text{NH}_2$  in chloroform. Each vibrational mode produces a pair of peaks along the diagonal that are separated by the anharmonicity of that mode, and each pair of modes gives two pairs of cross-peaks, one pair on either side of the diagonal, that are split by the coupling between those modes. In peptides, the anharmonicity and coupling are usually smaller than the linewidths, and thus the individual peaks in each pair are not resolved in the magnitude spectra. However, the peaks are resolved in the real part of the spectrum, because of their opposite signs. Molecules with sufficiently long vibrational lifetimes and larger splittings can have their 2D IR peaks completely resolved.<sup>21</sup> The cross peaks establish which peptide units are coupled and they enable the disentangling of multiple distributions of structures. For instance, the existence of some of the cross peaks in the IR-COSY spectrum of acetylproline- $\text{NH}_2$  in Fig. 4 shows that it adopts two separate distributions of structures in chloroform.

The coupling between the vibrational modes of each peptide unit can be measured from the intensities and frequencies of the cross peaks, which depend on the angular and spatial relations between the vibrational displacements. The angles can be measured independently by varying the polarization of the infrared pulses. An experiment of this type found that the two acetylproline- $\text{NH}_2$  structures have different mean angles between their vibrational dipoles.<sup>7</sup> The results indicate that the dihedral angles are close to those of an  $\alpha$ -helix for one of the distributions, and to an extended structure for the other. In wa-

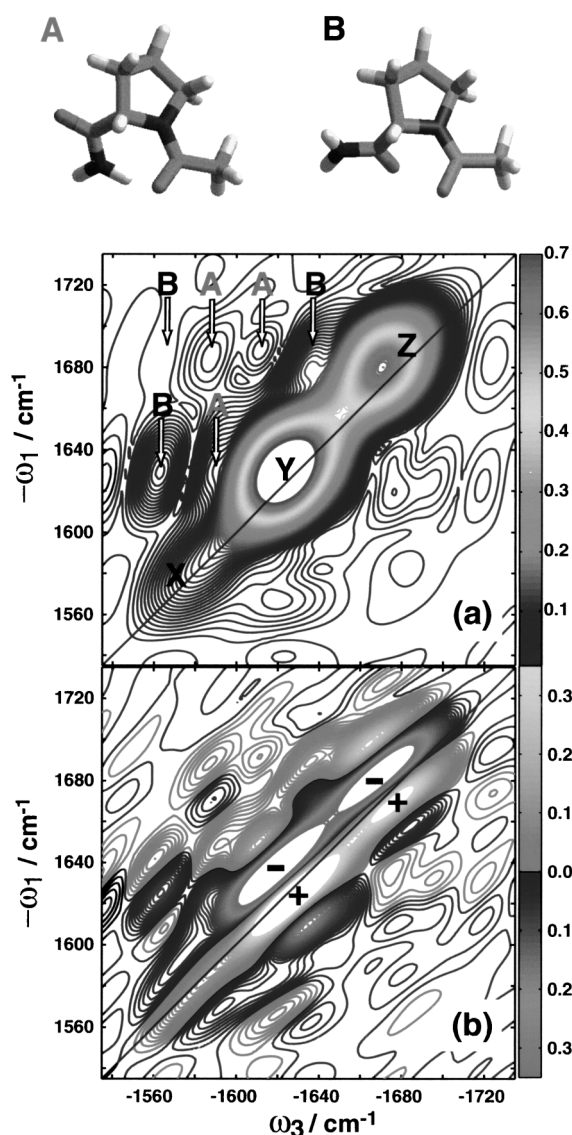


Fig. 4. The magnitude (a) and real (b) part of the heterodyned 2D IR (IR-COSY) spectra of acetylproline-NH<sub>2</sub> in chloroform.<sup>7</sup> The three diagonal peaks labeled X–Z in the magnitude spectra correspond to the three peaks in the linear spectrum (not shown) where peaks X and Z are from amide I and II vibrational modes that are located on the amino end of the molecule and peak Y is from the amide I mode on the acetyl end. Six cross-peaks are observed above the diagonal. Since three coupled modes should at most produce three pairs of cross peaks, acetylproline-NH<sub>2</sub> must adopt two conformations in chloroform. Comparison of a spectrum with all four pulses identically polarized to a spectrum with two of the infrared pulses polarized perpendicular to the other two determines the angles between the transition dipoles contributing to the respective peaks, which are related to the structures shown above (A and B). The cross-peaks are labeled with their respective structures. Each peak in the magnitude spectrum (a) has two peaks in the (b) real spectrum with opposite signs. The splittings between the peaks are a measure of the diagonal and off-diagonal anharmonicities of the modes, which are related to the couplings between the transition dipoles.

ter, only the extended structure with the two carbonyls hydrogen bonded to the solvent are observed in this spectrum. These conclusions about angles do not depend on the choice of inter-peptide potential energy function, although a potential is needed to find distances.

Molecular structures are generated from the measured angles and couplings by their dependence on the distances and angles between the transition charges of each peptide unit. The shapes of the peaks also depend on the vibrational dynamics of the system. Since the splitting between the pairs of cross-peaks is typically smaller than the line widths for peptides, it is important to understand the shapes of the peaks to accurately calculate the coupling and hence distances. A better understanding of the vibrational dynamics in peptides and proteins will thus lead to improved structural interpretation of the 2D IR spectra.<sup>50</sup>

Peptides and proteins will often have 2D IR spectra in which the diagonal and cross peaks overlap. One way to isolate specific residues and couplings is to use isotope labeling. Carbon-13 labeling the carbonyl carbon on the peptide backbone shifts the amide I frequency about 35 cm<sup>-1</sup> and allows the coupling between the labeled and unlabeled residues to be measured. This approach was used to study a 20-residue  $\alpha$ -helix to measure the coupling between different regions of the helix, and it was found that the spectra of the labeled peptides can be used to characterize the distribution of structures along the length of the peptide.<sup>6,51</sup>

#### Polarization Conditions

Each contribution to the third order nonlinear echo response depends on a fourth rank polar tensor that describes the orientation of the four molecule fixed transition dipole moments. From known properties of polar fourth rank tensors in isotropic media one can always express the general tensor element into terms that are the products of two factors, one that depends on the polarizations of the exciting fields and another that includes only the time dependent relative orientations of the dipoles (1). In isotropic media there are only three independent macroscopic observables obtainable from variations in the polarizations of the incident fields. Different linear combinations of the molecular tensor elements can be obtained by judicious choices of laboratory polarizations of the four pulses. Therefore the polarization conditions may be employed to examine specific microscopic contributions to the 2D IR spectrum. We have shown recently that the diagonal peaks can be eliminated from the spectra by choosing a sequence of polarized IR pulses.<sup>8</sup> As an example, the signal for a particular Feynman path that incorporates molecular based transition dipoles  $\alpha$ ,  $\beta$ ,  $\gamma$  then  $\delta$  in the four time step interaction with fields polarized  $\langle 45, -45, 90, 0 \rangle$  in the lab frame is given by:<sup>52</sup>

$$\langle \cos\theta_{\alpha\gamma}\cos\theta_{\beta\delta} - \cos\theta_{\alpha\delta}\cos\theta_{\beta\gamma} \rangle$$

In the case where two of the transition dipole directions in the molecule frame are involved in the interaction with the pulses, corresponding perhaps to excitations of two of the amide I groups in a peptide, this signal vanishes when the two transition dipoles are parallel ( $P_2 = 1$ ). Furthermore the diagonal contributions to the 2D IR spectrum vanish identically for this

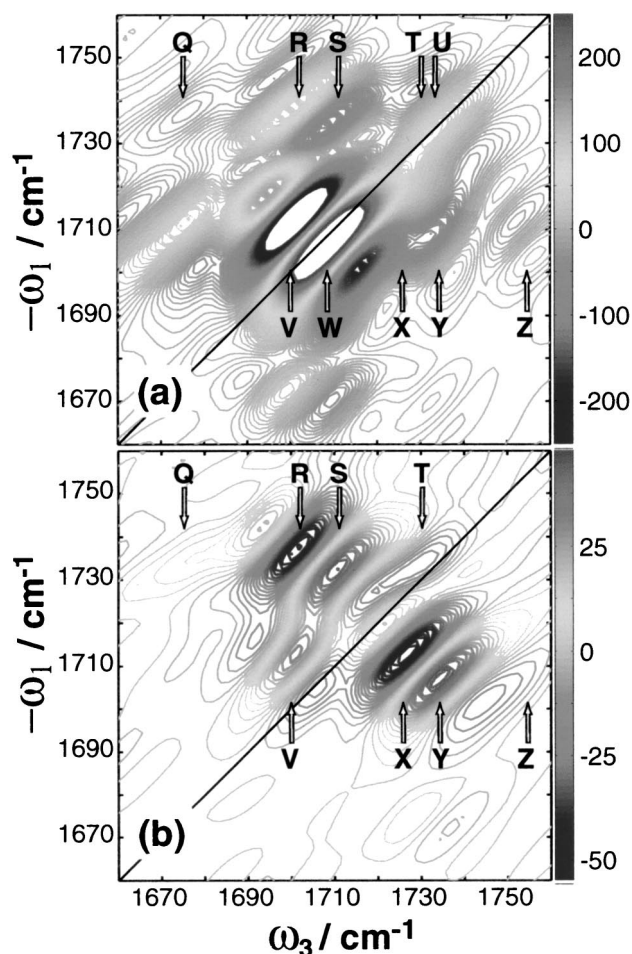


Fig. 5. The real part of the 2D IR spectrum of 1,3-cyclohexanedione for two polarizations: (a)  $\langle 0,0,0,0 \rangle$  and (b)  $\langle 45, -45, 90, 0 \rangle$ .<sup>8</sup> In (a), all 10 peaks predicted in Fig. 3 are observed, labeled Q–Z. The peaks T/U and V/W are the diagonal pairs, while the rest are cross peaks. Note that some cross peaks such as X and Y are obscured by the diagonal peaks in (a). In (b), the diagonal pairs are completely eliminated from the spectrum, and only the cross-peaks remain, which are now the dominant features. There still remains some intensity at T and V, which are due to transitions that are forbidden for extremely weak coupling.

polarization condition. This means that 2D IR spectra can be obtained free from the strong diagonal peaks and therefore contain only the cross peaks determined by the coupling between the pairs of modes (Fig. 5).

### Correlations

For coupled vibrators, the cross peaks in 2D spectra not only yield information on the geometric arrangements of the transition dipoles but also reveal the frequency correlation between the frequency distributions of the two vibrators because coherences on different vibrators are involved in the  $t_3$  and  $t_1$  evolution.<sup>9</sup> The occurrence of an echo is determined by whether the inhomogeneous distribution present during the interval  $t_3$  can rephase, which in turn depends on the correlation between the distributions involved in the  $t_3$  and  $t_1$  evolution. For example a conventional echo in a two level system depends on the

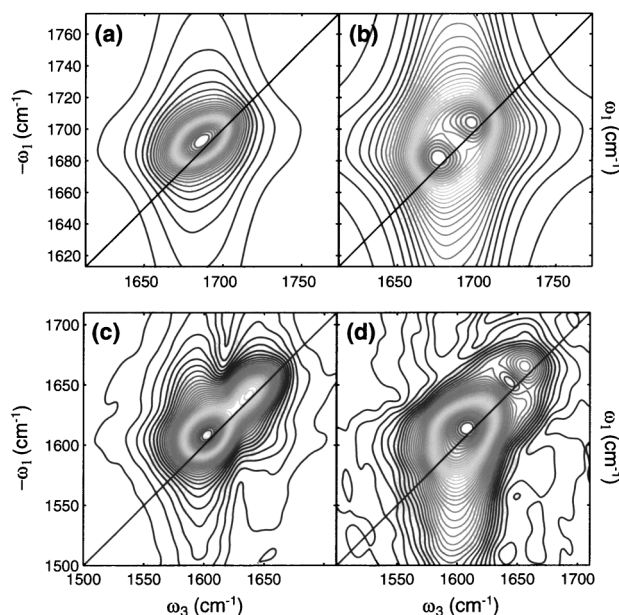


Fig. 6. Simulated absolute magnitude 2D rephasing (a) and nonrephasing (b) spectra for two independent vibrators at  $\omega_0^0 = 1700 \text{ cm}^{-1}$  and  $\omega_0^0 = 1686 \text{ cm}^{-1}$  with identical dynamical parameters. The two vibrators are closely spaced in frequency and they constructively interfere into a single unresolved peak in (a). However, they destructively interfere such that a valley appears in (b). This example illustrates that collecting 2D spectra in both quadrants may help to resolve closely spaced spectral features. The experimental absolute magnitude 2D rephasing (c) and nonrephasing (d) spectra for acetylproline-ND<sub>2</sub> in D<sub>2</sub>O show similar behavior as the above calculation for the amino amide I band, indicating the existence of two conformers.<sup>9</sup>

nonvanishing at  $t_3 = t_1$  of the frequency average  $\langle \exp[i\omega(t_1 - t_3)] \rangle$  where  $t_1$  is the delay between the excitation pulses. This result is dependent on the evolution of the Bloch vector being governed by the same distribution of frequencies during the intervals  $t_1$  and  $t_3$ . However in 2D IR spectra of vibrators, these distributions may be different so their correlation becomes crucial.<sup>9</sup> Both the lineshape and the intensity of the cross peaks depend on the frequency correlation between the two vibrators. In the rephasing spectra the cross peaks are pronounced and line-narrowed for positive correlation but broadened and diminished as the correlation becomes zero and negative. On the contrary, in the nonrephasing spectra the cross peaks are line-narrowed in the direction perpendicular to that in the rephasing spectra for negative correlation, but broadened as the correlation becomes zero or positive.<sup>9</sup> These results imply that the coupling strength between vibrators cannot be determined merely based on the cross peak intensities in a rephasing spectrum where the low intensities may result from negative correlations rather than from small coupling. Measuring rephasing and nonrephasing spectra separately is expected to provide more graphic information on coupling, correlation and structural distributions (Fig. 6).

### Simulations

Molecular dynamics simulations of the structural distribu-

tions and the associated amide-I vibrational modes were carried out for dialanine peptide in water and carbon tetrachloride.<sup>23</sup> The various manifestations in nonlinear infrared spectroscopy of the distribution of conformations of solvated dialanine were examined. In particular the simulations were used to predict the two-dimensional infrared spectroscopy of dialanine, which exhibits the coupling between the amide oscillators and the correlations of the frequency fluctuations. An internally hydrogen bonded conformation exists in  $\text{CCl}_4$  but not in  $\text{H}_2\text{O}$  where two externally hydrogen bonded forms are preferred. Simulations of solvated dialanine show how the 2D IR spectra expose the underlying structural distributions and dynamics that are not deducible from linear infrared spectra. In  $\text{H}_2\text{O}$  the 2D IR spectra shows cross peaks from large coupling in the alpha-helical conformer and an elongated higher frequency diagonal peak, reflecting the broader distribution of structures for the more flexible acetyl end. In  $\text{CCl}_4$ , the computed cross peak portion of the 2D IR spectra shows evidence of two amide I transitions in the high frequency region which are not apparent from the diagonal peak profile. The vibrational frequency inhomogeneity of the amide I band arises from fluctuations of the instantaneous normal modes of these conformers rather than the shifts induced by hydrogen bonding. Figure 7 shows the joint distribution of the acetyl and amino end frequencies in  $\text{H}_2\text{O}$ . The correlation coefficient between the two frequencies is found to be 0.3, indicating that the motions of two ends are uncorrelated on the average. However, the distribution shows distinct structure rather than a simple ellipsoidal shape with a long axis lying parallel to either axes, expected for a completely uncorrelated case. The detailed analysis of simulation shows that there are significant correla-

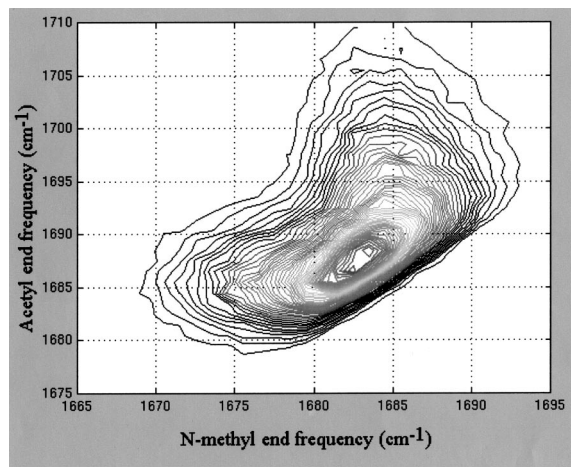


Fig. 7. The correlation between fluctuations of the amide I frequencies for the alanine dipeptide in water as calculated by molecular dynamics simulations. The overall correlation coefficient calculated from the illustrated distribution indicates that the two amide frequencies are uncorrelated. However, pieces of the inhomogeneous distributions are distinctly correlated as observed by the marked structure in the graph. In water, dialanine forms an extended structure where both ends are hydrogen bonded to the solvent. Systems that form an internal hydrogen bond may be more strongly correlated.

tions between fluctuations of the acetyl and amino end frequencies in  $\text{H}_2\text{O}$  that arise from mechanical coupling and not from hydrogen bonding at the two ends of the molecule.

### Energy Relaxation in Peptides

The IR-COSY experiment directly measures the dipolar couplings that depend on the inverse cube of the distances. On the other hand THIRSTY experiments<sup>7</sup> provide information on the transport of vibrational energy between the peptide units which, for electrostatic coupling, depends on the inverse sixth power of the distance.<sup>23</sup> Recently the intermode relaxation of acetylproline was reported using THIRSTY.

We have considered the theory of the dynamics of energy transfer between the two amide-I modes of dialanine.<sup>23</sup> The Redfield density matrix formalism provides the relationship of the energy transfer rate for a given site frequency difference and coupling in terms of their spectral densities. Molecular dynamics simulations have been utilized to obtain the site frequency gap and coupling spectral densities.<sup>23</sup> The coupling fluctuations have been shown to be statistically independent of the site frequency gap fluctuations. We find from such a calculation that the vibrational energy transfer between the amide-I modes is predicted to have time constant of 9 ps in  $\text{H}_2\text{O}$ . However, for an isotopomer, where the amino end frequency is further shifted down by  $35\text{ cm}^{-1}$ , we find the average rate constants to be significantly smaller (ns time scale). Thus, these calculations justify excluding the amide-I energy transfer from the calculations of the 2D IR spectra. At large site frequency separations the coupling fluctuations dominate the energy transfer rate whereas at small frequency separations, site frequency gap fluctuations dominate. Due to the correlation between the amide I frequencies from the amino and acetyl ends of the molecule, the frequency fluctuations that arise from internal coordinate motions do not influence the rate as much as those due to hydrogen bonding interactions. We also find the energy transfer rates to be different for different conformers of dialanine at small site frequency separations. Our recent measurements of acylproline have shown the dominant relaxation is not between the amide-I modes but involves their relaxation into the amide-II mode.<sup>53</sup>

### Conclusions

There are significant advantages in using 2D IR nonlinear methods, such as heterodyned echoes, rather than linear spectroscopies such as FTIR. These advantages include: (1) For  $N$  oscillators there is  $N(N + 1)/2$  times more information in the nonlinear infrared experiment compared with FTIR; (2) Coupling of modes necessary for structure determination can be obtained directly and free from models in 2D IR; (3) Properties of potentials such as the diagonal and off-diagonal anharmonicities are measured directly in the 2D IR experiment but not in FTIR. The complexity of linear IR spectra in the overtone and combination band regions is greatly reduced in 2D IR which is naturally a double resonance experiment; (4) The various dynamical contributions to the vibrational spectra are directly measured in 2D IR. While linear IR measures only the dipole correlation function the 2D IR measures the frequency correlation functions of the oscillators, their orientational and population relaxation and the inhomogeneous distributions.

The inhomogeneous distributions and the correlations between them are also observables of 2D IR while FTIR cannot dissect the lineshapes in this manner. Population and coherence transfer can be measured in 2D IR but is not detectable in FTIR.

However there are currently some limitations of nonlinear IR, the most important of which is the difficulty of generating phase controlled femtosecond pulses of IR radiation over the complete range needed to study all modes of interest. This limitation will soon be removed by advances in laser technology and experimental design. The challenge of determining small signals in the presence of a heterodyne field is common to both techniques.

So far 2D IR has been applied to small molecules and peptides. Extension to larger systems is now underway. The 2D IR spectroscopy provides a combination of structure sensitivity and time resolution. It promises to become a powerful technique in determining distributions of structures that are averaged out in NMR, such as the random coil state of proteins or the transient opening of membrane channels. The methods are immediately employable as structural probes of kinetic processes that can be initiated with light pulses such as protein folding or chemical reactions, and may become the method of choice for monitoring distributions of complex molecular assemblies evolving on hitherto unprecedented timescales. There are many variants of 2D IR and higher dimensional IR spectroscopies to be explored and applied to problems in areas of condensed matter dynamics where knowing how structures change in time will be important. Therefore the field looks very promising indeed.

This research was supported by the National Institutes of Health, the National Science Foundation, and Research Resource NIHRR-13456, and an NIH NSRA fellowship to M.T.Z. (1 F32 GM20462-01).

## References

- 1 P. Hamm, M. Lim, and R. M. Hochstrasser, *J. Phys. Chem. B*, **102**, 6123 (1998).
- 2 P. Hamm, M. Lim, W. F. DeGrado, and R. M. Hochstrasser, *Proc. Natl. Acad. Sci. U.S.A.*, **96**, 2036 (1999).
- 3 P. Hamm, M. Lim, W. F. DeGrado, and R. M. Hochstrasser, *J. Chem. Phys.*, **112**, 1907 (2000).
- 4 M. C. Asplund, M. T. Zanni, and R. M. Hochstrasser, *Proc. Natl. Acad. Sci. U.S.A.*, **97**, 8219 (2000).
- 5 M. T. Zanni, M. C. Asplund, and R. M. Hochstrasser, *J. Chem. Phys.*, **114**, 4579 (2001).
- 6 M. T. Zanni, M. C. Asplund, S. M. Decatur, and R. M. Hochstrasser, in "Ultrafast Phenomena XII," ed by T. Elsaesser, S. Mukamel, M. M. Murnane, and N. F. Scherer, Springer-Verlag, Berlin (2000), pp. 504-506.
- 7 M. Zanni, S. Gnanakaran, J. Stenger, and R. M. Hochstrasser, *J. Phys. Chem. B*, **105**, 6520 (2001).
- 8 M. T. Zanni, N.-H. Ge, Y. S. Kim, and R. M. Hochstrasser, *Proc. Natl. Acad. Sci. U.S.A.*, **98**, 11265 (2001).
- 9 N.-H. Ge, M. T. Zanni, and R. M. Hochstrasser, *J. Phys. Chem. A*, (2002), **106**, 962 (2002).
- 10 Mukamel, S., "Principles of nonlinear spectroscopy," Oxford Univ. Press, New York, (1995).
- 11 W. M. Zhang, V. Chernyak, and S. Mukamel, *J. Chem. Phys.*, **110**, 5011 (1999).
- 12 S. Mukamel, *Annu. Rev. Phys. Chem.*, **51**, 691 (2000).
- 13 C. Scheurer, A. Piryatinski, and S. Mukamel, *J. Am. Chem. Soc.*, **123**, 3114 (2001).
- 14 J. D. Hybl, A. W. Albrecht, S. M. Gallagher-Faeder, and D. M. Jonas, *Chem. Phys. Lett.*, **297**, 307 (1998).
- 15 G. R. Fleming and M. Cho, *Annu. Rev. Phys. Chem.*, **47**, 109 (1996).
- 16 J. P. Likforman, M. Joffre, and V. Thierry-Mieg, *Opt. Lett.*, **22**, 1104 (1997).
- 17 V. Astinov, K. J. Kubarych, C. J. Milne, and R. J. D. Miller, *Chem. Phys. Lett.*, **327**, 334 (2000).
- 18 S. Woutersen and P. Hamm, *Springer Ser. Chem. Phys.*, **66**, 499 (2001).
- 19 S. Woutersen and P. Hamm, *J. Chem. Phys.*, **114**, 2727 (2001).
- 20 S. Woutersen and P. Hamm, *J. Phys. Chem. B*, **104**, 11316 (2000).
- 21 O. Golonzka, M. Khalil, N. Demirdoven, and A. Tokmakoff, *Phys. Rev. Lett.*, **86**, 2154 (2001).
- 22 A. Piryatinski, S. Tretiak, V. Chernyak, and S. Mukamel, *J. Raman Spec.*, **31**, 125 (2000).
- 23 S. Gnanakaran and R. M. Hochstrasser, *J. Am. Chem. Soc.*, **123**, 12886 (2001).
- 24 W. Zhao and J. C. Wright, *Phys. Rev. Lett.*, **84**, 1411 (2000).
- 25 R. M. Hochstrasser, P. Hamm, M. Lim, N.-H. Ge, and W. F. DeGrado, *Biophys. J.*, **78**, 76Plat (2000).
- 26 M. Gulotta, R. Gilmanshin, T. C. Buscher, R. H. Callender, and R. B. Dyer, *Biochemistry*, **40**, 5137 (2001).
- 27 K. D. Rector, J. W. Jiang, M. A. Berg, and M. D. Fayer, *J. Phys. Chem. B*, **105**, 1081 (2001).
- 28 M. Lim, P. Hamm, and R. M. Hochstrasser, *Proc. Natl. Acad. Sci. U.S.A.*, **95**, 15315 (1998).
- 29 P. Hamm, M. Lim, W. F. DeGrado, and R. M. Hochstrasser, *J. Phys. Chem. A*, **103**, 10049 (1999).
- 30 D. E. Sagnella, J. E. Straub, T. A. Jackson, M. Lim, and P. A. Anfinsen, *Proc. Natl. Acad. Sci. U.S.A.*, **96**, 14324 (1999).
- 31 S. Krimm and J. Bandekar, *Adv. Protein Chem.*, **38**, 181 (1986).
- 32 H. Torii and M. Tasumi, *J. Chem. Phys.*, **96**, 3379 (1993).
- 33 H. Torii, T. Tatsumi, and M. Tasumi, *Mikrochim. Acta Suppl.*, **14**, 531 (1997).
- 34 S. H. Lee and S. Krimm, *Chem. Phys.*, **230**, 277 (1998).
- 35 K. Palmo and S. Krimm, *J. Comput. Chem.*, **19**, 754 (1998).
- 36 B. Mannfors, K. Palmo, and S. Krimm, *J. Mol. Struct.*, **556**, 1 (2000).
- 37 W. Qian and S. Krimm, *J. Phys. Chem.*, **101**, 5825 (1997).
- 38 T. C. Cheam and S. Krimm, *Chem. Phys. Lett.*, **107**, 613 (1984).
- 39 N. G. Mirkin and S. Krimm, *J. Am. Chem. Soc.*, **113**, 9742 (1991).
- 40 Special Issue: *Chem. Phys.* **266**, 135-368 (2001).
- 41 A. Tokmakoff and M. D. Fayer, *J. Chem. Phys.*, **103**, 2810 (1995).
- 42 P. Hamm, M. Lim, and R. M. Hochstrasser, *Phys. Rev. Lett.*, **81**, 5326 (1998).
- 43 P. Hamm, M. Lim, M. Asplund, and R. M. Hochstrasser, *Chem. Phys. Lett.*, **301**, 167 (1999).

- 44 M. C. Asplund, M. Lim, and R. M. Hochstrasser, *Chem. Phys. Lett.*, **323**, 269 (2000).
- 45 K. A. Merchant, D. E. Thompson, and M. D. Fayer, *Phys. Rev. Lett.*, **86**, 3899 (2001).
- 46 N. Demirdoven, M. Khalil, O. Golonzka, and A. Tokmakoff, *J. Phys. Chem. A*, **105**, 8025 (2001).
- 47 A. Seilmer and W. Kaiser, in "Ultrashort laser pulses", ed by Kaiser, W. Springer-Verlag, New York, (1993) p. 279.
- 48 J. C. Owrutsky, D. Raftery, and R. M. Hochstrasser, *Ann. Rev. Phys. Chem.*, **45**, 519 (1994).
- 49 L. K. Iwaki and D. D. Dlott, *J. Phys. Chem. A*, **104**, 9101 (2000).
- 50 A. Piryatinski, V. Chernyak, and S. Mukamel, *Chem. Phys.*, **266**, 285 (2001).
- 51 S. M. Decatur, *Biopolymers*, **54**, 180 (2000).
- 52 R. M. Hochstrasser, *Chem. Phys.*, **266**, 273 (2001).
- 53 I. Rubstov and R. M. Hochstrasser, *J. Phys. Chem.*, in press.